

Characterization of Ultrasound Tactile Display

Georgios Korres and Mohamad Eid^(✉)

Department of Engineering, New York University Abu Dhabi,
Saadiyat Island, United Arab Emirates
{george.korres,mohamad.eid}@nyu.edu

Abstract. Traditional haptic interfaces require physical contact between the haptic device and the user. An elegant and novel solution is to provide contactless tactile stimulation via airborne acoustic radiation pressure. However, the characteristics of contactless tactile displays are not well studied in the literature. In this paper, we study the characteristics of the ultrasonic tactile display as a haptic interface. In particular, we examine the effects of increasing the number of ultrasound transducers on four characteristics, namely the maximum producible force, the workspace, the workspace resolution, and the robustness of the simulation. Three rectangular-shaped 2D array configurations are considered: single-tile (10×10 transducers), two-tiles (10×20 transducers), and four-tiles (20×20 transducers). Results show that the maximum producible force remains almost constant as the number of tiles increases, whereas the elevation at which these maxima are generated increases. The workspace increases along the xy-plane as the number of tiles increase almost linearly, however, the elevation of the workspace remains almost the same. Finally, we found that the robustness of tactile display decreases as the number of tiles increases.

Keywords: Haptic interfaces · Ultrasound transducer array · Tactile display

1 Introduction

Haptic-based ultrasonic stimulation relies on an airborne acoustic phased array for giving tactile sensation at the human skin [5]. Dalecki et al. demonstrated that tactile sensations could be evoked from the ultrasound radiated on the skin in water [4]. Subsequent research by Shinoda and colleagues expanded further on this concept, using 2D array of ultrasonic transducers, to produce one focal point on the submerged hand [14]. The study suggested using ultrasound at 40 kHz; higher frequency resulted in higher energy attenuation and degradation in spatial resolution of focusing.

Shinoda and colleagues studied airborne ultrasound tactile stimulation to enhance the quality of the tactile stimulation and integrate it with visual display. A feasibility study with 91 transducers was conducted to generate a fixed focal point [16]. To animate the focal point and produce higher tactile forces

of around 16 mN (20 mm spatial resolution and 1 kHz vibrations), a subsequent work extended the tactile display to 324 transducers [12]. Experiments showed that users were able to discriminate tactile stimulation movement direction. A further development with 2,241 transducers offered a much larger workspace of 1 m^3 and an improved temporal resolution of 0.5 ms [8]. The system was then integrated with a touch screen to enable noncontact blind touch interaction by adding tactile feedback for notifying the finger location [23,24]. A recent study by Inoue et al. produced a spatially stationary haptic image using ultrasonic waves to construct 3D haptic images without depending on sensor feedback for tracking the hand position [13].

Gavrilov presented a method to display 2D tactile shapes by generating multiple focus ultrasonic focal points [7]. This method led to the development of UltraHaptics; a multi-point tactile feedback system with an interactive visual screen [2]. They further improved the technology for rendering 3D volumetric haptic shapes [19]. A similar work for rendering volumetric tactile shapes via ultrasound is demonstrated in [17]. Displaying haptic texture via ultrasound is demonstrated in [3,21].

Several researchers tried to improve the quality of tactile displays by varying the characteristics of the ultrasonic system (increasing the number of transducers, work-space, producible forces, etc.). For instance, an approach is presented for measuring the strength of the ultrasonic pressure field in [11]. A spatial resolution of less than 0.1 mm with a total force of 16 mN is measured on a 2-D cross-sectional area of $180 \times 180 \text{ mm}$ at 200 mm elevation above the array surface, with 18×18 discrete focal point positions. The radiation pressure field of a system comprising of two ultrasonic transducers with different radiation frequencies is analyzed in [18]. Hoshi characterized an aerial tactile system with two arrays of 96 transducers each and a target workspace of $200 \times 200 \times 200 \text{ mm}$ (divided into $5 \times 5 \times 12.5 \text{ mm}$ sub-areas). Each of these sub-areas can be a target focal point that can stimulate tactile feedback in mid-air [9]. The output force for each array is 12 mN.

Existing work has reported varying and sometimes conflicting results about the characteristics of ultrasonic tactile display devices. For instance, [15,16] reported 8 mN of output force at 250 mm elevation, a haptic rendering frequency of 1 KHz, and 20 mm of spatial resolution with 91 transducers. The authors in [10] utilized 364 transducers to achieve 47 mN of output force at 250 mm of elevation, a spatial resolution of 20 mm, and an unmeasured workspace. Hoshi et al. measured 16 mN at 200 mm of elevation, rendering frequency of 1 KHz, and 20 mm of spatial resolution using 324 transducers [11,12]. Multiple ultrasound transducer arrays were deployed in [8,22] with 2241 transducers in total to generate 73 mN of output force at 600 mm elevation, a rendering frequency of 1 kHz, and a spatial resolution of 20 mm. Hoshi reported 12 mN of output force at 300 mm elevation, a rendering frequency of 1 kHz, and 36.4 mm spatial resolution with 384 transducers [9]. Yoshino and Shinoda built a tactile visio-acoustic screen with 249 ultrasound transducers to generate 16 mN of output force at 240 mm elevation and a 10 mm spatial resolution [23]. Other research

in the acoustic manipulation technology returned similar results. For instance, graphics can be generated using levitated small objects carried by ultrasound pressure [20]. The study reported a spatial resolution of 0.5 mm, a workspace of 270 mm along the z-axis, and a producible force of 20 mN.

In this paper we present an experimental platform for measuring the characteristics that define the quality of the ultrasound tactile display as a haptic interface. The remainder of the paper is organized as follows: Sect. 2 presents an overview of the tile-based Haptogram system that is used in the experimental study. Section 3 presents the experimental setup, procedure, and results along with a discussion of the derived characteristics. Section 4 summarizes our findings.

2 Haptogram System

2.1 Haptogram System Overview

The Haptogram system is presented thoroughly in our previous work [6]. The Haptogram system architecture comprises a software subsystem and a hardware subsystem as shown in Fig. 1(a). The software subsystem has three components: Graphical User Interface (GUI), 3D Point Cloud Representation (PCR) and Focal Point Calculation (FPC). The GUI, shown in Fig. 1(b), enables users to create tactile objects that can be displayed (2D or 3D objects). The PCR component converts the model into a point cloud of focal points, with timestamps representing the order in which these focal points must be displayed. The FPC component calculates the distances between each focal point and the transducers, and the timings to produce the focal point at the desired 3D location. The software subsystem is generalized for N-tiles. The timings for all the $N \times 100$ transducers are calculated automatically.

Three components make up the hardware subsystem, as shown in Fig. 1(a): the FPGA Controller, the Driver Circuit Amplification (DCA) component and the Ultrasound Array (UA). The FPGA Controller produces synchronized pulse signals that feed into the DCA. The DCA component is an amplifier circuit that

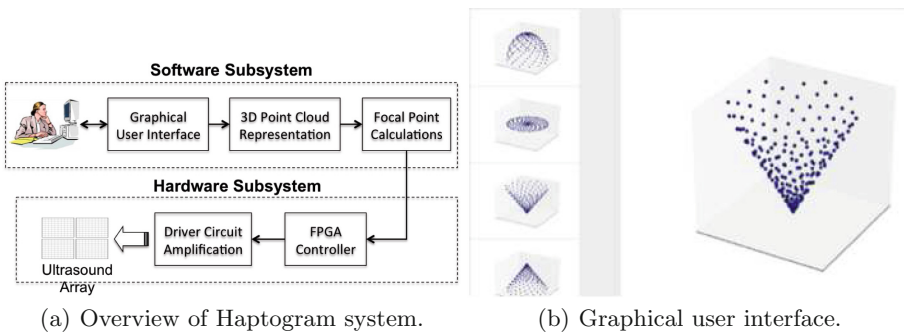


Fig. 1. Haptogram system.

produces sufficient currents to drive the ultrasound transducers. The UA is a composition of tiles of a two-dimensional array of ultrasound transducers (a tile includes 10×10 transducers).

2.2 3D Tactile Rendering

The Haptogram system renders point-cloud 3D tactile objects by switching focal points at a frequency up to 1.34 KHz. The flowchart explaining the haptic rendering is shown in Fig. 2. First of all, the tile configuration is loaded (N number of tiles, n number of transducers along x-axis, and m number of transducers along y-axis) along with the 3D point cloud file that represents the 3D tactile object to be displayed. Then, the coordinates of each focal point (x,y,z) are used to determine all the distances between the given focal point and every transducer of the tiled array ($N \times 100$ transducers). Next, the distances are used to calculate the timings needed by each transducer to produce ultrasound waves. Finally the timings are stored in a HEX memory file that can be uploaded to the FPGA boards.

2.3 The Tile-Based Ultrasonic Array

The fundamental building block of the UA component is a two-dimensional array of ultrasound transducers (10×10 transducers). The MA40S4S 40 kHz Murata ultrasound transducer is used with 10 mm size diameter, 120 dB sound pressure, 80° directivity, and 20 Vpp allowable input voltage. As the number of tiles varies with different Haptogram system configurations, it is imperative for the interaction system to adapt so that users can have a nearly consistent experience regardless of the system configuration. Haptogram is a modular system so that multiple tiles can be connected and used without the need to change the application software.

The hardware architecture for the N-tiles design is shown in Fig. 3(a). The synchronization for the N tiles work as follows: First, the master FPGA will immediately fire the driver circuit to drive its own transducers and create the sequence of focal points. The master FPGA will send a SYNC = 1 pulse to the

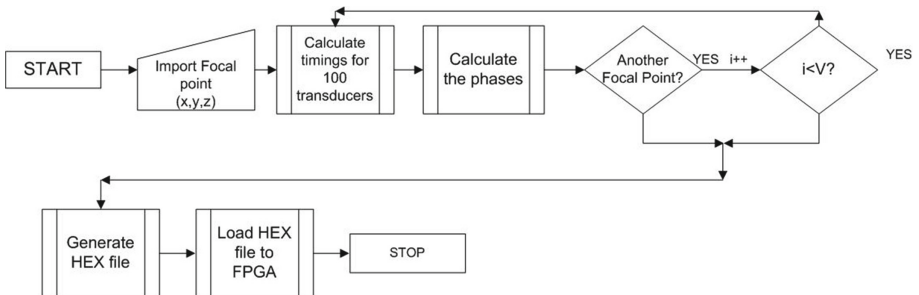


Fig. 2. 3D point cloud haptic rendering for the N tiles Haptogram system.

first slave FPGA once an entire cycle of focal points execution is completed. Then, the first slave FPGA resets the execution of its focal points so that on the next cycle both the master tile and slave tile 1 are synchronized. The same procedure takes place to synchronize slave tile 2 with slave tile 1, and so on.

3 Characterization of the Haptogram System

This section presents an experimental study to determine the haptic characteristics of the tile-based Haptogram system as the number of tiles increases. Specifically, we will focus on characteristics that define the quality of the system as a haptic interface, namely the maximum producible forces, the device workspace, workspace resolution and display robustness. We will compare these characteristics for three configurations: single-tile configuration, two-tiles configuration, and four-tiles configurations.

3.1 Experimental Setup

In order to measure the spatial distribution of the acoustic radiation pressure, we used the experimental setup shown in Fig. 3(b). An ultrasonic sensor probe was attached to the end effector of the robotic arm (ST Robotics R17) whose resolution for movement is 0.1 mm. The sound probe is an MA40S4S 40 kHz Murata ultrasound transducer. Its output was fed to AC-to-DC conversion circuit (a rectifying bridge followed by an array of decoupling capacitors). The resulting DC signal is fed to a 10-bit Analog to Digital Converter (ADC). Finally the digital output is calibrated for force measurement in mN. The following settings were also used in this experiment: the current is limited to 900 mA whereas the voltage is limited to ± 12 V.

A simple script is developed to control movement of the robotic arm to measure the force distribution in an arbitrary 3D volume on top of the ultrasound array. Measurement data is acquired at a 1 kHz rate. At every position, 20 sample measurements are taken; the average is stored as the tactile stimulation force at that position to reduce the random noise.

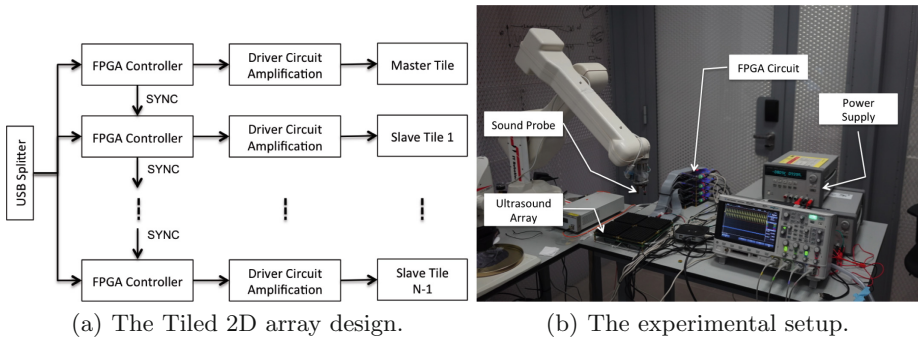


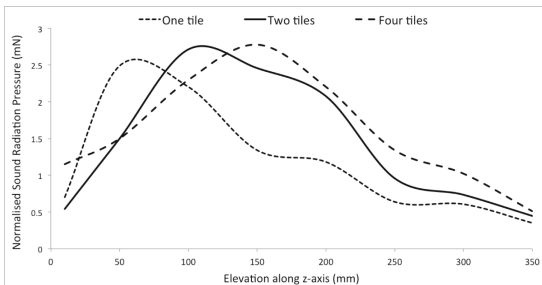
Fig. 3. Tile-based Haptogram.

3.2 Maximum Producible Force

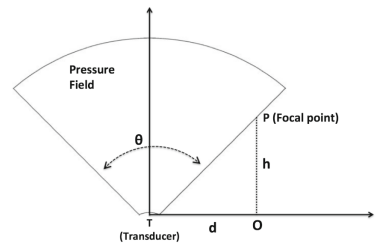
The most important characteristic of a haptic device is its ability to produce perceivable forces. In this experiment, the aim is to study how the maximum producible force is affected by an increase in the number of tiles. The robotic arm scans the workspace along the z-axis, starting from an elevation of 20 mm to 350 mm, with a step size of 2 mm. Fourteen (14) focal point stimulations are generated, from an elevation of 40 mm to 300 mm with a step size of 20 mm. For each focal point, for instance (0,0,40 mm), the robotic arm is used to scan the z-axis from 20 mm to 350 mm to measure the acoustic pressure along the z-axis. In total, 14 sets of data are generated where each peak value represents the maximum producible force corresponding to each focal point. The peaks for these data sets are plotted in Fig. 4(a). Similar measurements are made along both the x-axis (from -150 mm to $+150$ mm) and the y-axis (from -150 mm to $+150$ mm). The same procedure is performed for the three tile configurations.

Fig. 4(a) shows that as the number of tiles increases, the maximum producible force remains almost the same in terms of amplitude (around 2.73 mN). However the elevation at which the maximum force is produced increases. The maximum forces produced for the one-tile, two-tiles, and four-tiles configurations are found at 76 mm, 120 mm, and 155 mm respectively. The shift in the location of the maximum force is explained by the limited directivity of the transducers. In order for a transducer to contribute to a focal point, the minimum height of the focal point is defined as $h = d \tan \frac{\pi - \theta}{2}$ see Fig. 4(b). In Fig. 4(b), θ is the transducer directivity, d is the distance from the center of the array to transducer, F is the focal point location, T is the transducer location, and h is the elevation at which the focal point is formed.

The height at which the furthest transducers contributes are calculated as follows (for the single-tile configuration): $h = \alpha \frac{\sqrt{2}}{2} \tan(50^\circ) = 76$ mm. Similarly, the heights for two tiles are four tiles configurations are 119.0 mm and 151.6 mm. These values are consistent with the experimental results as demonstrated in Figs. 4(a) and 5. As the elevation increases beyond these heights the pressure decreases due to the attenuation of the acoustic waves.



(a) Force distribution along the z-axis.



(b) Minimum height for a transducer contribution.

Fig. 4. Acoustic pressure field.

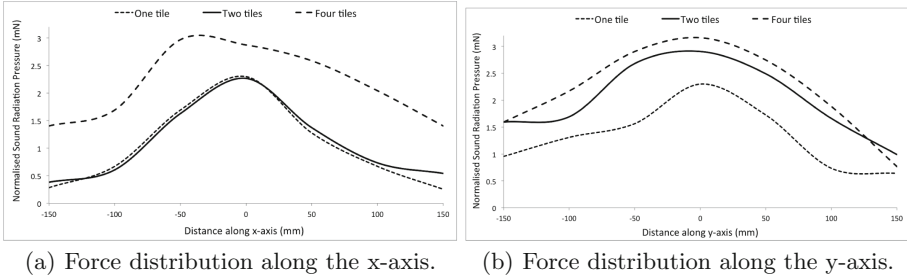


Fig. 5. Acoustic pressure field along xy-plane.

Figure 5(a) shows the force distribution along the x-axis and Fig. 5(b) shows the force distribution along the y-axis. These graphs are utilized to derive the effective workspace for the various configurations. For instance, along the x-axis it is clear that the workspace for the one-tile is almost the same as the workspace for the two-tiles configuration since the two-tiles configuration is aligned along the y-axis (workspace of around 100 mm). Table 1 shows the maximum producible forces for each configuration. It is clear that as the number of tiles increase, the maximum producible force remains almost the same. This is justifiable due to the fact that as the number of tiles increases, further transducers would have less contribution due to limited directivity of the transducers.

Table 1. Maximum producible forces for three tile configurations.

	Single-tile	Two-tiles	Four-tiles
Dimensions (transducers)	10×10	10×20	20×20
Maximum Forces (mN)	2.49	2.52	2.55

3.3 Workspace

One of the key characteristics in any haptic device which limits its applicability as a haptic display is the achievable workspace. In order to quantify the tile-based workspace, the robotic arm scanned a volume of $300 \times 300 \times 300 \text{ mm}^3$ on top of the array with a step size of 1 mm^3 to measure the effective workspace. For each measurement point, the Haptogram is instructed to generate a focal point at the measurement point, then 20 readings are made and the average value is recorded.

Since a wide variety of parameters could influence stimulus detection at the palm (such as duration, frequency, temporal modulation), we defined the workspace based on the amplitude threshold of the generated force. The detectability of a stimulus is defined as the threshold value above which observers

can detect the stimulus more than 50 % of its occurrences. A pilot study is conducted with the experimental setup where the threshold is found to be 2 mN. Therefore, if the average force generated at this measurement point is higher than 2.0 mN, the measurement is plotted onto the workspace graph with a color code proportional to the corresponding intensity.

Figure 6 show the generated graphs of the workspace for the three tile configurations. First of all, we observe that the workspace is symmetrical around the three orthogonal axes, with a workspace in the form of a skewed ellipsoid. Secondly, the workspace volume is increasing linearly as the number of tiles increase. Finally, even though the maximum producible forces remained constant across the three configurations, the workspace volume is elevated along the z-axis as the number of tiles increase. It is clear from Fig. 6 that the center of the workspace is elevated from 76 mm for one-tile configuration to 120 mm for 2-tiles configuration to 155 mm for the 4-tiles configuration. These results are explicitly shown in Table 2. This is mainly due to the fact that the transducers can better reach and contribute to focal point located at higher elevations due to the limited directivity.

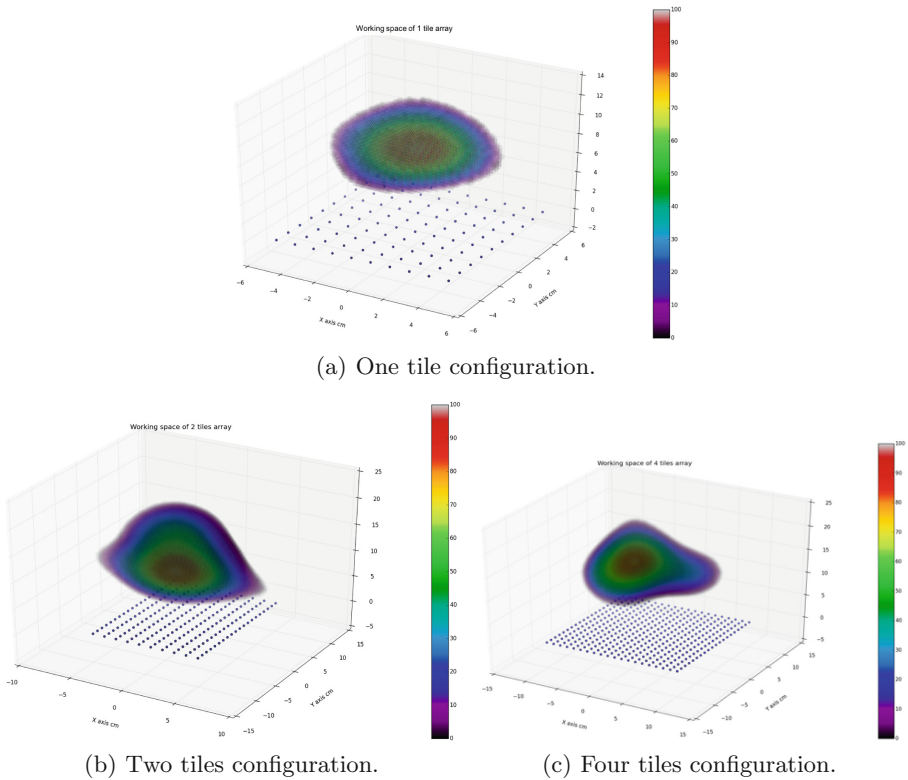


Fig. 6. Workspace for three tile configurations.

Table 2. Workspace volume for the three configurations.

	Single-tile	Two-tiles	Four-tiles
Number of transducers	10×10	10×20	20×20
Workspace (mm^3)	$110 \times 110 \times 110$	$110 \times 220 \times 180$	$250 \times 270 \times 180$
Workspace center (mm)	(0,0,76)	(0,0,120)	(0,0,155)

3.4 Stimulation Robustness

Another interesting characteristic is the stimulation robustness. The stimulation robustness is defined as the ability of the Haptogram system to display consistently the forces it is instructed to display. To evaluate stimulation robustness, the average and standard deviation of the forces generated within the device workspace are measured (shown in Table 3) for several trials of tactile stimulation. Results show that as the number of tiles increases, the average forces remain almost the same. However, the standard deviation for the generated forces increases as the number of tiles increase. This implies that as the number of tiles increases, the ability of the Haptogram system to reproduce forces consistently and robustly decreases. This is probably due to the increased ultrasound radiation (as the number of transducers increase), which results in a noticeable increase in the ultrasonic noises due to multiple reflections and interference.

Table 3. Average and standard deviation of tactile forces for the three tile configurations.

	Single-tile	Two-tiles	Four-tiles
Average (mN)	2.36	2.26	2.12
Standard Deviation (mN)	0.13	0.26	0.43

3.5 Discussion

The experimental analysis has clearly demonstrated the ability of airborne acoustic radiation to generate perceivable tactile stimulation. The one-tile configuration was able to generate an average force of 2.36 mN (standard deviation of 0.13 mN), over an elevation range of 8 cm to 15 cm.

The airborne acoustic radiation technology has several advantages as a tactile display. First of all, the temporal bandwidth is broad enough to produce 3D tactile feelings by generating a sequence of tactile focal points and switching between them at a high frequency (1.63 KHz for 200 focal points configuration). Secondly, the spatial resolution is good enough (5 mm diameter of a focal point) to produce various 2D and 3D shapes, as reported in a previous study about tactile stimulation at the palm [1].

Even though the maximum producible force marginally increases as the number of tiles increases, the elevation at which these maxima are generated increases

(76 mm for one-tile, 120 mm for 2-tiles, and 150 mm for 4-tiles). This implies that for certain applications where point-based or 2D stimulation is desirable (such as displaying a virtual typing pad), an increase in the number of tiles would shift higher the ideal elevation for tactile stimulation. In case of 3D tactile stimulation, this is less important since any focal point within the stimulation workspace is palpable.

The display workspace increases along the xy-plane almost linearly as the number of tiles increase. However the center of the workspace is shifted higher as the number of tiles increase. This raises a question of whether the utilized transducers are best suited for this kind of application or whether a novel design must be considered to improve the quality of tactile stimulation. The power consumption for the whole tiled system is another factor that must be considered, particularly if applications with mobile devices are to be pondered on.

As for the workspace resolution, the Haptogram system is capable of producing high number of focal points and is thus capable of presenting high-resolution 3D tactile objects. For instance, the single tile configuration is capable of producing a maximum of 10,648 focal points within a workspace of $110 \times 110 \times 110 \text{ mm}^3$, where the dimensions of one focal point are $5 \times 5 \times 5 \text{ mm}^3$. As for the two tiles and four tiles configurations, the total number of focal points is 34,848 and 97,200 respectively.

4 Conclusion

In this paper, we presented a study to characterize the airborne ultrasound technology as a tactile display using the Haptogram system. A performance analysis is presented to measure the impact of increasing the number of transducers on the maximum producible forces, the display workspace, the workspace resolution, and stimulation robustness. As a result, it is confirmed that an increase in the number of transducers: (1) does not noticeably increase the maximum producible force but shifts it higher, (2) stretches workspace along the xy-directions, and shift the center of the workspace higher along the z-axis, (3) significantly increases the spatial resolution of the tactile display, and (4) decreases the stimulation robustness.

References

1. Bickley, L., Szilagui, P.: *Bates' Guide to Physical Examination and History Taking*, 9th edn. Lippincott Williams and Wilkins, Philadelphia (2007)
2. Carter, T., Seah, S., Long, B., Drinkwater, B., Subramanian, S.: Ultrahaptics: multi-point mid-air haptic feedback for touch surfaces. In: 26th Annual ACM Symposium on User Interface Software and Technology, pp. 505–514 (2013)
3. Ciglar, M.: An ultrasound based instrument generating audible and tactile sound. In: Conference on New Interfaces for Musical Expression (NIME 2010), pp. 10–22 (2010)
4. Dalecki, D., Child, S., Raeman, C., Carstensen, E.: Tactile perception of ultrasound. *J. Acoust. Soc. Am.* **97**, 3165–3170 (1995)

5. Ebbini, E., Cain, C.: Multiple-focus ultrasound phased-array pattern synthesis: optimal driving-signal distributions for hyperthermia. *IEEE Trans. Ultrason. Ferroelectr. Freq. Control* **36**, 540–548 (1989)
6. Eid, M.: Haptogram: aerial display of 3D vibrotactile sensation. In: *IEEE International Conference on Multimedia and Expo Workshops*, pp. 1–5 (2014)
7. Gavrilov, L.: The possibility of generating focal regions of complex configurations in application to the problems of stimulation of human receptor structures by focused ultrasound. *Acoust. Phys.* **54**, 269–278 (2008)
8. Hasegawa, K., Shinoda, H.: Aerial display of vibrotactile sensation with high spatial-temporal resolution using large-aperture airborne ultrasound phased array. In: *World Haptics Conference*, vol. 2013, pp. 31–36 (2013)
9. Hoshi, T.: Development of aerial-input and aerial-tactile-feedback system. In: *IEEE World Haptics Conference*, pp. 569–573 (2011)
10. Hoshi, T., Abe, D., Shinoda, H.: Adding tactile reaction to hologram. In: *IEEE International Symposium on Robot and Human Interactive Communication*, pp. 7–11 (2009)
11. Hoshi, T., Iwamoto, T., Shinoda, H.: Non-contact tactile sensation synthesized by ultrasound transducers. In: *Third Joint Symposium on Haptic Interfaces for Virtual Environment and Teleoperator Systems*, pp. 256–260 (2009)
12. Hoshi, T., Takahashi, M., Iwamoto, T., Shinoda, H.: Noncontact tactile display based on radiation pressure of airborne ultrasound. *IEEE Trans. Haptics* **3**, 155–165 (2010)
13. Inoue, S., Makino, Y., Shinoda, H.: Active touch perception produced by airborne ultrasonic haptic hologram. In: *IEEE World Haptics Conference (WHC)*, pp. 362–367 (2015)
14. Iwamoto, T., Shinoda, H.: Two-dimensional scanning tactile display using ultrasound radiation pressure. In: *IEEE Proceedings of HAPTICS*, vol. 46, pp. 57–61 (2006)
15. Iwamoto, T., Tatzono, M., Hoshi, T., Shinoda, H.: Airborne ultrasound tactile display. In: *35th International Conference and Exhibition on Computer Graphics and Interactive Techniques*, p. 1 (2008)
16. Iwamoto, T., Tatzono, M., Shinoda, H.: Non-contact method for producing tactile sensation using airborne ultrasound. In: Ferre, M. (ed.) *EuroHaptics 2008*. LNCS, vol. 5024, pp. 504–513. Springer, Heidelberg (2008)
17. Long, B., Seah, S., Carter, T., Subramanian, S.: Rendering volumetric haptic shapes in mid-air using ultrasound. *ACM Trans. Graph.* **33**(6), 181 (2014)
18. Masy, S., Tangen, T., Standal, Ø., Deibele, J., Nasholm, S., Hansen, R., Angelsen, B., Johansen, T.: Nonlinear propagation acoustics of dual-frequency wide-bandexcitation pulses in a focused ultrasound system. *J. Acoust. Soc. Am.* **128**(5), 2695–2703 (2010)
19. Nishino, H., Goto, R., Kagawa, T., Yoshida, K., Utsumiya, K., Hirooka, J., Osada, T., Nagatomo, N., Aoki, E.: Design with tactile feedback. In: *International Conference on Complex, Intelligent and Software Intensive Systems*, pp. 53–60 (2011)
20. Ochiai, Y., Hoshi, T., Rekimoto, J.: Pixie dust: graphics generated by levitated and animated objects in computational acoustic-potential field. *ACM Trans. Graph.* **33**, 85 (2014)
21. Shiokawa, Y., Tazo, A., Konyo, M., Maeno, T.: Hybrid display of realistic tactile sense using ultrasonic vibrator and force display. In: *IEEE/RSJ International Conference on Intelligent Robots and Systems*, pp. 3008–3013 (2008)
22. Takahashi, M., Shinoda, H.: Large aperture airborne ultrasound tactile display using distributed array units. In: *SICE Annual Conference*, pp. 359–362 (2010)

23. Yoshino, K., Shinoda, H.: Visio-acoustic screen for contactless touch interface with tactile sensation. In: World Haptics Conference (WHC), pp. 419–423 (2013)
24. Yoshino, K., Shinoda, H.: Contactless touch interface supporting blind touch interaction by aerial tactile stimulation. In: Haptics Symposium (HAPTICS), pp. 347–350 (2014)